ICINCO 2025

22nd International Conference on Informatics in Control, Automation and Robotics

PROCEEDINGS

Volume 1

Marbella, Spain 20 - 22 October, 2025

EDITORS

Giuseppina Carla Gini Radu-Emil Precup Dimitar Filev

https://icinco.scitevents.org

SPONSORED BY

INSTICC

PAPERS AVAILABLE AT



ICINCO 2025

Proceedings of the 22nd International Conference on Informatics in Control, Automation and Robotics

Volume 1

Marbella - Spain

October 20 - 22, 2025

Sponsored by

INSTICC - Institute for Systems and Technologies of Information, Control and Communication

IEEE Technically co-sponsored by IEEE SMC - TC on Evolving Intelligent Systems

Technically Co-sponsored by IFAC - International Federation of Automatic Control

ACM In Cooperation
SIGAI - ACM Special Interest Group on Artificial Intelligence

In Cooperation with

AAAI - Association for the Advancement of Artificial Intelligence INNS - International Neural Network Society

Copyright © 2025 by SCITEPRESS – Science and Technology Publications, Lda.

Edited by Giuseppina Gini, Radu-Emil Precup and Dimitar Filev

Printed in Portugal ISSN: 2184-2809

ISBN: 978-989-758-770-2

DOI: 10.5220/0000205300003982

Depósito Legal: 551123/25

https://icinco.scitevents.org icinco.secretariat@insticc.org

CONTENTS

INVITED SPEAKERS

KEYNOTE SPEAKERS	
Towards Transparent, Physically Consistent Machine Learning Models Robert Babuska	
Dealing with "Dirty" Data: Solutions from Fuzzy Systems Research	

Data Aware Agentic AI: Cognitive, Control, and Data Flows

Michael Berthold

9

INTELLIGENT CONTROL SYSTEMS AND OPTIMIZATION

FULL PAPERS

Uzay Kaymak

Enhancing Pharmaceutical Batch Processes Monitoring with Predictive LSTM-Based Framework Daniele Antonucci, Davide Bonanni, Domenico Palumberi, Luca Consolini and Gianluigi Ferrari	15
A Novel Automatic Monitoring and Control System For Induced Jet Breakup Fabrication of Ceramic Pebbles Miao Zhang, Oliver Leys, Markus Vogelbacher, Regina Knitter and Jörg Matthes	25
Health-Aware Charging of Li-Ion Batteries Using MPC and Bayesian Degradation Models Taranjitsingh Singh, Jeroen Willems, Bruno Depraetere and Erik Hostens	37

Manipulation of Deformable Linear Objects Using Model Predictive Path Integral Control with Bidirectional Long Short-Term Memory Learning

47

Lukas Zeh, Johannes Meiwaldt, Zexu Zhou, Armin Lechler and Alexander Verl

Reinforcement Learning for Model-Free Control of a Cooling Network with Uncertain Future Demands

Jeroen Willems, Denis Steckelmacher, Wouter Scholte, Bruno Depraetere, Edward Kikken,

Abdellatif Pay Tamagagai and Ann Nové

Approximating MPC Solutions Using Deep Neural Networks: Towards Application in Mechatronic

Approximating MPC Solutions Using Deep Neural Networks: Towards Application in Mechatronic Systems

Edward Kikken, Jeroen Willems, Branimir Mrak and Bruno Depraetere

Optimal Camera Placement for 6D Head Pose Estimation

Harshita Soni, Nikhil Tirumala and Aratrik Chattopadhyay

82

Dual-Arm Manipulation of a T-Shirt from a Hanger for Feeding a Hem Sewing Machine Filipe Almeida, Gonçalo Leão, Carlos M. Costa, Cláudia D. Rocha, Armando Sousa, 93 Lara Gomes da Silva, Luís F. Rocha and Germano Veiga

Solving the Three-Dimensional Beacon Placement Problem Using Constraint-Based Methods, Large Neighborhood Search, and Evolutionary Algorithms 105 Sven Löffler, Viktoria Abbenhaus, George Assaf and Petra Hofstedt

71

5

7

Place Recognition with Omnidirectional Imaging and Confidence-Based Late Fusion Marcos Alfaro, Juan José Cabrera, Enrique Heredia, Oscar Reinoso, Arturo Gil and Luis Paya	117
Continual Multi-Robot Learning from Black-Box Visual Place Recognition Models Kenta Tsukahara, Kanji Tanaka, Daiki Iwata, Jonathan Tay Yu Liang and Wuhao Xie	126
Enhancing Resilience of Strong Structural Controllability in Leader-Follower Networks Vincent Schmidtke and Olaf Stursberg	136
Predictive Quality of In-Fabrication Products in Smart Manufacturing Using Graph-Based Deep Learning Peter Davison, Muhammad Fahim, Roger Woods, Scott Fischaber, Marcus Haron and Cormac McAteer	145
Application of MPPT Techniques Using Intelligent and Conventional Control Strategies João T. Sousa and Ramiro S. Barbosa	154
SHORT PAPERS	
Time-Optimal Scheduling of Tasks with Shared and Dynamically Constrained Energy Systems <i>Eero Immonen</i>	169
Leader-Follower Coordination in UAV Swarms for Autonomous 3D Exploration via Reinforcement Learning Robert Kathrein, Julian Bialas, Mohammad Reza Mohebbi, Simone Walch, Mario Döller and Kenneth Hakr	176
Translating NWP Outputs into UAV-Specific Predictions Using Machine Learning David Sládek	184
Mobile Application with Convolutional Neural Networks for the Early Detection of Diseases in Blueberry Plants in Chepén: Trujillo Santiago Sebastian Heredia Orejuela and Aaron Moises Cosquillo Garay	192
Observation-Based Inverse Kinematics for Visual Servo Control Daniel Nikovski	200
Evaluation Approaches for an Aggregated Meteorological Model for Artillery Operations Jan Ivan, Viktor Vitoul, Ladislav Potužák and Jan Drábek	208
Categorical Model Estimation with Feature Selection Using an Ant Colony Optimization Tetiana Reznychenko, Evženie Uglickich and Ivan Nagy	219
Vision-Based Autonomous Landing for the MPC Controlled Fixed Wing UAV Sevinç Günsel, Şeref Naci Engin and Mustafa Doğan	227
Enhancing PI Tuning for Plant Commissioning Using Transfer Learning and Bayesian Optimization Boulaid Boulkroune, Joachim Verhelst, Branimir Mrak, Bruno Depraetere, Joram Meskens and Pieter Bovijn	235
Towards Scalable and Fast UAV Deployment Tim Felix Lakemann and Martin Saska	243
Real-Time Weld Quality Prediction in Automated Stud Welding: A Data-Driven Approach Beatriz Coutinho, Bruno Santos, Rita Gomes Mendes, Gil Gonçalves and Vítor H. Pinto	251

Quantitative Analysis of Ambient Temperature Effects on Steptime Variations in Industrial Pneumatic Actuators Jon Zubieta, Unai Izagirre and Luka Eciolaza	259
Data-Driven Control of a PEM Electrolyzer Yeyson A. Becerra-Mora, Juan Manuel Escaño and José Ángel Acosta	267
An Educational Platform for Real-Time Control and Reinforcement Learning Experiments Using Rotary Inverted Pendulum and LW-RCP Doyoon Ju, Jongbeom Lee and Young Sam Lee	274
Automated Process Control for the Beam Gas Curtain Vacuum System at CERN L. Cantu, R. Ferreira, J. Francisco Rebelo, A. Rocha, C. Vazquez Pelaez and L. Zygaropoulos	282
Hierarchical Coordination of UAVs for Dynamic Task Assignment in Large-Scale Traffic Surveillance Missions Teewende Boris kiema, Hélène Piet-Lahanier, Najett Neji and Samia Bouchafa	290
Intelligent Process Automation Model for Credit Campaign Management Optimization in a Financial Institution Fernando Schilder Hervias and Neil Trujillo Nerya	298
Smart Water Management: Integrating PLC and SCADA Technologies for Sustainable Urban Infrastructure Nirmal Kumar Balaraman, Krunal Patel and Nagender Reddy	305
A Robust Comparative Study of Adaptative Reprojection Fusion Methods for Deep Learning Based Detection Tasks with RGB-Thermal Images Enrique Heredia-Aguado, Marcos Alfaro-Pérez, María Flores, Luis Paya, David Valiente and Arturo Gil	313
Balancing Speed and Accuracy: A Comparative Analysis of Segment Anything-Based Models for Robotic Indoor Semantic Mapping Bruno Georgevich Ferreira, Armando Jorge Sousa and Luis Paulo Reis	321
Satellite Navigation Constellation Optimisation Problem Definition for the Application of Genetic Algorithms Paula Piñeiro Ramos, Sebastian Bernhardt, Helena Stegherr and Jörg Hähner	329
Recursive Gaussian Process Regression with Integrated Monotonicity Assumptions for Control Applications Ricus Husmann, Sven Weishaupt and Harald Aschemann	340
Real-Time Fault Detection and Diagnosis for Oil Well Drilling Using a Multitask Neural Network <i>Marios Gkionis, Ole Morten Aamo and Ulf Jakob Flø Aarsnes</i>	350
Improving Assistive Technologies Using EEG Headsets David Ivaşcu and Isabela Drămnesc	362
Kalman Type Filtering in the Presence of Parametric Modeling Uncertainties: A Navigation System Application for Launch Vehicles <i>Adrian-Mihail Stoica</i>	369
Pedestrian Positioning Technology Combining IMU and Wireless Signals Based on MC-CKF Seong Yun Cho and Jae Uk Kwon	375

Adaptive Trajectory Prediction in Roundabouts Using Moving Horizon Estimation Selsabil Bougherara, Hasni Arezki, Chouki Sentouh, Jérôme Floris and Jean-Christophe Popieul	380
Combining off-Policy and on-Policy Reinforcement Learning for Dynamic Control of Nonlinear Systems	387
Ahmed A. Hani Hazza, Simon G. Fabri, Marvin K. Bugeja and Kenneth. Camilleri	301
SIGNAL PROCESSING, SENSORS, SYSTEMS MODELLING AND CONTROL	
FULL PAPER	
Filtering of Polytopic-Type Uncertain State-Delayed Noisy Systems Eli Gershon	399
SHORT PAPERS	
Space-Filling Regularization for Robust and Interpretable Nonlinear State Space Models Hermann Klein, Max Heinz Herkersdorf and Oliver Nelles	409
Wind Farm Power Prediction Using a Machine Learning Surrogate Model from a First-Principles Simulation Model Sebastian E. Pralong, Samuel Martínez-Gutiérrez, Dan E. Kröhling, Alejandro Merino, Gonzalo E. Alvarez, Daniel Sarabia and Ernesto C. Martínez	417
Experimental Evaluation of Camouflage Effectiveness Against Ground-Based Surveillance Viktor Vitoul, Jan Ivan, Ladislav Potužák, Michal Šustr and Barbora Hanková	425
Verifying Positivity of Piecewise Quadratic Lyapunov Functions Sigurdur Hafstein and Eggert Hafsteinsson	435
Video-Based Vibration Analysis for Predictive Maintenance: A Motion Magnification and Random Forest Approach	
Walid Gomaa, Abdelrahman Wael Ammar, Ismael Abbo, Mohamed Galal Nassef, Tetsuji Ogawa and Mohab Hossam	445
Towards Machine Learning Driven Virtual Sensors for Smart Water Infrastructure Vineeth Maruvada, Karamjit Kaur, Matt Selway and Markus Stumptner	453
Unsupervised Analysis of Cyclist Performance for Route Segmentation and Ranking Rensso Mora-Colque and William Robson Schwartz	461
Sky Savers: Leveraging Drone Technology for Victim Localization in Avalanche Rescue via Transceiver Signal Analysis Robin Vetsch, Samuel Kranz, Tindaro Pittorino, Peter de Baets, Martial Châteauvieux, Christoph Würsch, Daniel Lenz and Sebastien Gros	469
Optimizing Sensor Deployment Strategy for Tracking Mobile Heat Source Trajectory Thanh Phong Tran, Laetitia Perez, Laurent Autrique, Edouard Leclercq, Syrine Bouazza and Dimitri Lefevbre	477
Robust LiDAR-Based Parking Slot Detection and Pose Estimation for Shell Eco-Marathon Vehicles <i>Miklós Unger and Ernő Horváth</i>	486
From Algebraic Synthesis and GRAFCET to Logical Controller Design in ST Code (IEC 61131-3) Mathieu Roisin, Dimitri Renard, David Annehicane, Bernard Riera and Pierre-Alain Yvars	494

Adaptive Output Control with a Guarantee of the Specified Control Quality Nikita Kolesnik	502
On the Synthesis of Stable Switching Dynamics to Approximate Limit Cycles of Nonlinear Oscillators <i>Nils Hanke, Zonglin Liu and Olaf Stursberg</i>	509
An Adaptive-Robust Strategy Design for Process Control Dumitru Popescu, Catalin Dimon and Pierre Borne	517
High-Level Synthesis of an Efficient Hardware Implementation for a Smart Tactile Sensing System <i>María-Luisa Pinto-Salamanca, Wilson-Javier Pérez-Holguín and José Antonio Hidalgo-López</i>	524
Estimation of Rate-Dependent Hammerstein Model of Piezo Bender Actuator Lenka Kuklišová Pavelková	532
AUTHOR INDEX	539

A Robust Comparative Study of Adaptative Reprojection Fusion Methods for Deep Learning Based Detection Tasks with RGB-Thermal Images

Enrique Heredia-Aguado^{©a}, Marcos Alfaro-Pérez^{©b}, María Flores^{©c}, Luis Paya^{©d}, David Valiente^{©e} and Arturo Gil^{©f}

University Institute for Engineering Research, Miguel Hernández University, Avda. de la Universidad s/n, 03202 Elche (Alicante), Spain

Keywords: Image Fusion, Multispectral Image, Object Detection, RGB-Thermal, Deep Learning.

Abstract:

Fusing visible and thermal imagery is a promising approach for robust object detection in challenging environments, taking advantage of the strengths from different spectral information. Building on previous work in static early fusion, we present a comparative study of adaptative reprojection fusion methods that exploit advanced projections and frequency-domain transforms to combine RGB and thermal data. We evaluate Principal Component Analysis, Factor Analysis, Wavelet and Curvelet-based fusion, all integrated into a YOLOv8 detection pipeline. Experiments are conducted on the LLVIP dataset, with a focus on methodological rigour and reproducibility. This research show promising results based on these methods comparing to previous early fusion methods. We discuss the implications for future research and the value of robust experimental design for advancing the state of the art in multispectral fusion.

1 INTRODUCTION

Multimodal data fusion has consistently demonstrated its value across various knowledge domains. By combining different sources of information, it is possible to compensate for the limitations of individual modalities and take advantage their complementary strengths.

The primary application scenario for this research is object detection in search and rescue (SAR) operations, surveillance, and security domains, contexts where robust perception under uncontrollable conditions is critical. The proposed solution is designed for deployment onboard autonomous robotic platforms, requiring real-time processing capabilities under hardware constraints. While high-frequency inference is not mandatory, achieving reliable performance at rates around 1 Hz is sufficient to support effective operations.

Visible (RGB) images provide rich texture and colour information, but their performance signifi-

- ^a https://orcid.org/0009-0001-7717-1428
- ^b https://orcid.org/0009-0008-8213-557X
- ° https://orcid.org/0000-0003-1117-0868
- d https://orcid.org/0000-0002-3045-4316
- e https://orcid.org/0000-0002-2245-0542
- f https://orcid.org/0000-0001-7811-8955

cantly degrades under poor illumination. In some scenarios this limitation can be addressed with artificial lighting; however, in the scenarios considered here, such approach is not feasible. To ensure robust performance under highly varying illumination conditions, data fusion emerges as a promising strategy to enhance perception. Thermal infrared images, less sensitive to illumination changes, provide complementary information about temperature and emissivity. Specifically, the long-wave infrared spectrum offers temperature measurements between 0 and 100°C, depending on camera settings, which is particularly suitable for pedestrian detection. However, thermal images are sensitive to environmental changes, such as ambient temperature and seasonal variations. As described in (Heredia-Aguado et al., 2025), there are corner cases—such as occlusions present in only one modality—that further justify the integration of both data sources.

As indicated before, visible spectrum image include rich information about textures, colour and image structure, while thermal image adds light invariance. Effective fusion should exploit these complementary characteristics to improve object detection in low-light or visually degraded environments. Beyond the domains already mentioned, multispectral fusion has potential applications in other fields as well.

Several fusion strategies exist in the literature. This research builds upon static early fusion techniques (Heredia-Aguado et al., 2025) to establish a robust baseline for comparing the benefits of various approaches. Specifically, the fusion methods explored in this work reduce a four-channel image (RGB+T) to a three-channel representation, enabling the use of established image detectors such as YOLOv8. This paper extends the study of static early fusion techniques by:

- Proposing and rigorously evaluating dynamic fusion methods based on projections (PCA, FA) and frequency-domain transforms (Wavelets, Curvelets).
- Ensuring robust experimental control: using the same dataset, network architecture, initialization, and training parameters across all methods.

The following Section (2) details the methodology employed, including the detection algorithm, dataset, experimental setup, and evaluation metrics. Section 3 explains each fusion method. Section 4 presents and discusses the detection results for each approach. Finally, Section 5 summarizes the main findings, limitations, and potential future directions.

2 METHODOLOGY

The fusion algorithms that are tested in this research combine both thermal and visible spectrum images before they are fed to train and validate a deep learning model to perform the detection for each specific fusion approach, as shown in Figure 1. This section includes a detailed description of each block depicted in Figure 1 along with an explanation of the relevant experimental setup and the evaluation metrics that will be involved in the later analysis and discussion.

For the sake of reproducibility, the source code is openly available (https://github.com/enheragu/yolo_test_utils/tree/v2.1.0-icinco, accessed on 01 July 2025), allowing for complete replication of the experiments.

2.1 Detection Algorithm

All the fusion algorithms included in this research have been tested under the same detection network. The idea of the network is to work as a common descriptor of how each method performs. For this purpose YOLOv8 (Jocher et al., 2023) have been selected. YOLO is a state-of-the-art single-stage object detection architecture that unifies both localiza-

Table 1: LLVIP test and train subset characteristics.

-	Set Name	Images	Backgrounds	Instances	
	Test	3463	0	8302	
	Train	12,025	2	34,135	

tion and classification within a single neural network. Although it efficiently extracts multi-scale features in three different sizes, it is a known issue that the detection may suffer with smaller objects that disappear through the convolution layers (Jiang et al., 2022) (Diwan et al., 2023).

Although there are other detectors that could potentially overcome these issues, the use case domain in which this research is focused need a fast and low-cost consuming solution. In terms of speed YOLOv8 has proven to be faster than the other state-of-the-art family of solutions based on RCNN Networks such as Faster-RCNN (Ren et al., 2017). Although there are detection models based on transformers (Carion et al., 2020) these models are still quite big in terms of trainable parameters and memory consumption. YOLOv8 offers a reliable solution with a fast processing time and low memory and trainable parameters, implying a shorter training time and the need for smaller datasets.

2.2 The LLVIP Dataset

For this research the LLVIP dataset (Jia et al., 2021) has been chosen. It includes up to 16 k colourthermal image pairs with pedestrians manually labelled, captured at night under low illumination conditions. Images provided (1280 x 1024) have been captured with a static pair of cameras in 26 different locations. The dataset is already provided with a 80-20 split for train/test subsets. As summarised in Table 1 the images have been labelled and filtered so that all pedestrians are identified removing almost all only-background images. This dataset seems to be one of the most reliable datasets in terms of multiespectral images. Although bigger datasets such as the KAIST (Hwang et al., 2015) dataset exist, they have not the quality in terms of image pair alignment (Heredia-Aguado et al., 2025) and labelling as LLVIP. Note that the fusion methods proposed are dependant on the alignment of both visible and thermal images and that problems in calibration or synchronization between images can greatly impact the performance of the methods.

Examples of both test and training subsets are shown in Figure 2. As can be observed, all the images have been taken from a high-angle perspective, which means that most people appear relatively close to the camera, maintaining a consistent size and avoiding smaller instances that, as already stated, would neg-

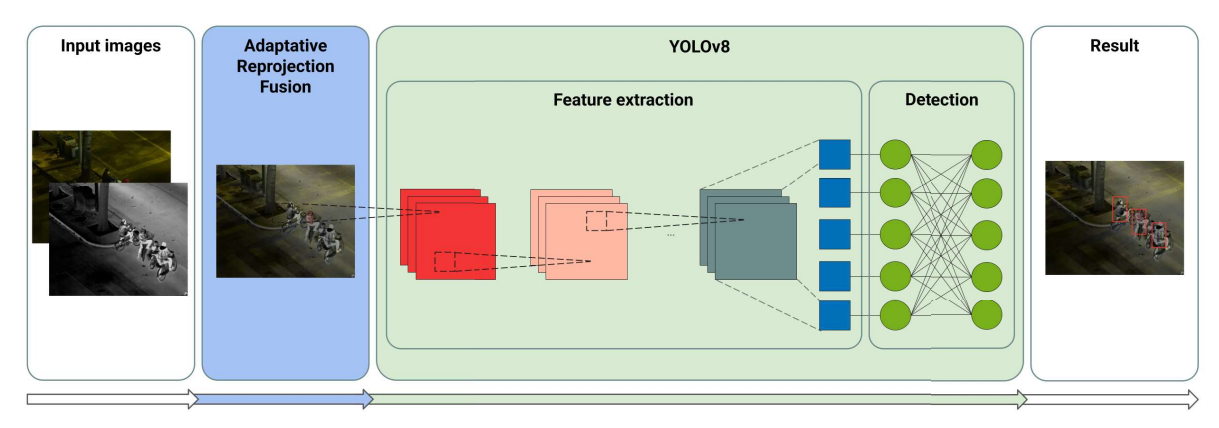


Figure 1: Architectural design for the fusion algorithm evaluation.

atively affect the detection algorithm.



Figure 2: LLVIP examples from test and train subsets.

2.3 Experimental Setup

As already stated, the idea of this research is to establish a comparison framework between different fusion methods. As some of them (middle fusion, late fusion) imply changes in the deep-model architecture, no transfer learning is to be used. All the models are trained from scratch, making use of the resulting fused images, and based on the same initialization weights and identical hyperparameters, including data augmentation strategies, and initialization schemes. This guarantees a robust and fair comparison across the different fusion algorithms

All the training and validation tests were performed using the same hardware: an NVIDIA GPU, model GeForce RTX 4090 with 24 GB. The adaptative fusion of each image is done in a 11th Gen Intel(R) Core(TM) i7-11700 (2.50GHz) processor.

2.4 Evaluation Metrics and Implementation Details

To have a clearer understanding of the performance and focusing on the use case already presented, the performance of each method will be compared based on the precision and recall metrics. Precision provides a measure of the ability of the trained model to avoid false positives while recall informs about the capacity of the model to detect all instances without leaving undetected ones.

The analysis also includes the standard metric mean Average Precision (mAP) at standard IoU (Intersection over Union) thresholds. Fusion time is also reported for each method, as computational efficiency is critical for real-time applications.

3 IMAGE FUSION

The fusion methods that are presented cover different alternatives of reprojecting the four channel information into a three channel output. The first couple of methods are based on reprojecting the data into a different frame based on data variation. The following methods include fusion in the frequency domain before data are reprojected back to the three-channel format.

This section covers PCA and FA as methods of dimensionality reduction applied to image fusion; and Wavelet and Curvelet transform for image fusion. Other alternatives tested such as t-SNE (Van der Maaten and Hinton, 2008) or UMAP (McInnes et al., 2020) may take up to 40 minutes of computation time for each image, which is completely out of the scope of the current research use case domain.

As already introduced, these resulting images are then fed to the deep detection network, YOLOv8, to train and validate the resulting model.

3.1 Projection-Based Fusion

3.1.1 Principal Component Analysis (PCA)

Principal Component Analysis involves a mathematical tool that transforms a given number of correlated variables into a number of uncorrelated variables. With this approach, and starting with four-channel data, through PCA the maximum variance directions are computed. Taking the most relevant components (three components in this case), the image is backprojected to the image space. This method has been proposed with different variants and applications in the field of image processing (Kumar and Muttan, 2006) (Elmasry et al., 2020).

For this research the generic approach is followed, for each image the data are reprojected based on the three most relevant components and then fed to the deep-learning algorithm.

3.1.2 Factor Analysis (FA)

Following a similar approach to the PCA tool, Factor Analysis is another tool for dimensionality reduction based on data variance (Joliffe and Morgan, 1992). With this tool a set of factors are computed (similar to components in PCA), so that the input variables are assumed to be linear combinations of these factors plus, for each variable, an error term. The key advantage of the method is that it allows the separation of the common variance in the data from the variance attributable to error. This way, the reprojection is made only through the factors computed based on common variance. Although it is not a method commonly used in image processing, we think it brings some interesting approach to the problem as noise or even outliers are not an unknown thing in image processing.

3.2 Frequency-Domain Fusion

3.2.1 Wavelet Transform Fusion

The Discrete Wavelet Transform (DWT) (Sifuzzaman et al., 2009) is a derived technique based on the Fourier Transform. The Fourier transform analyses a given signal based on its frequency components, but in doing so, it loses spatial information about the data. Two-dimension DWT ensures maintaining spatial information (critical when analysing an image) while focusing on the frequency analysis (Zhang, 2019). With this approach a given image can be decomposed into frequency components.

For each channel of the four-channel input image, the DWT provides a set of frequency components. These components are splitted into two subbands: approximation coefficients (cA) and detail coefficients sub-bands. These coefficients are the ones mixed between images: RGB approximation coefficient is mixed with thermal approximation coefficient; the same applies to the detail coefficients. Once fused, an inverse transform is applied to reconstruct a three-channel image.

The detail sub-bands, the high frequency component of the image, capture mainly local changes, textures and edges information, while approximation sub-bads, the low frequency components, contain most of the general structure and spectral image information. There are different approaches on how these components should be combined:

- Maximum value: Between two given components the maximum value is maintained disregarding the other one. This approach ensures maintaining texture and edge information, but it can include higher noise in the resulting image.
- Average value: Although averaging both components can diminish local changes and edges, it maintains a smoother and cleaner image.

Both versions have been implemented into two Wavelet fusions: averaged and max-value. For the first version the components of each RGB channel are averaged with the ones from the thermal image, for both approximation and detail sub-bands. The second approach combines each RGB channel detail components with the thermal components keeping the maximum value. In this case the approximation coefficient is combined following an α Blending Fusion (Ofir, 2023): $C_{Aprox} = \alpha \cdot C_{A-RGB} + (1 - \alpha) \cdot C_{A-TH}$ being alpha a relative coefficient based on thermal pixel value. The max-value method tends to preserve more information than the average method in image fusion, as it selects the highest intensity pixel from the input images, ensuring that no significant details from any source are lost, whereas averaging can dilute or blur important features (Patil et al., 2013) (Sahu and Sahu, 2014). Other techniques that show interesting results are based on max-contrast (Indira, 2015) but have not been tested as would potentially increase time consumption.

3.2.2 Curvelet Transform Fusion

The problem with the Wavelet transformation is that it focuses on point singularities, ignoring some of the geometric properties of the structures in the image. In addition, it does not take advantage of edge regularity (Ma and Plonka, 2010). The Curvelet trans-

form defines a different transform from the DWT, as it performs a multi-scale and multi-directional analysis that is particularly effective when representing and compressing edge and curve structures. Not surprisingly, it is widely popular for image processing solutions (Starck et al., 2002).

As in the DWT fusion approach, two versions of the algorithm have been implemented. In both, the first layer coefficients are merged averaging both RGB and Thermal coefficients. In the last levels (up to four levels in total) are either averaged or maximum-filtered.

In Figure 3 an example of each fusion for a given image is presented. As it can be observed both the FA and the Curvelet fusion provide a cleaner solution with regards to the PCA and Wavelet fusion, better isolating the instance and relevant information from the image. Although visually subtle, the max-value version of each method (DWT or Curvelet) tends to provide a clearer image (in a similar way to the differences between DWT and Curvelet fusion results). It can be depicted on Figure 4d, deliberately cropped and enlarged to pixel level, how the maximum-value fusion tends to miss some information and produce noisier results with regards to the average version.

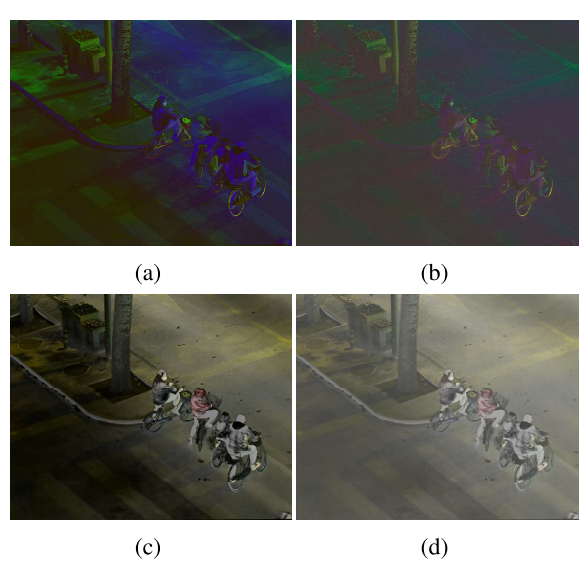


Figure 3: Examples in false colour representation of the result of each fusion method based on an LLVIP dataset image. (a) PCA fusion. (b) FA fusion. (c) Wavelet based fusion (averaged channels). (d) Curvelet based fusion (averaged channels).

For reproducibility purposes, the source code of both reprojection methods (https://github.com/enheragu/yolo_test_utils/blob/v2.1.0-icinco/src/Dataset/fusion_methods/pca_fa_compression.py, accessed on 01 July 2025)

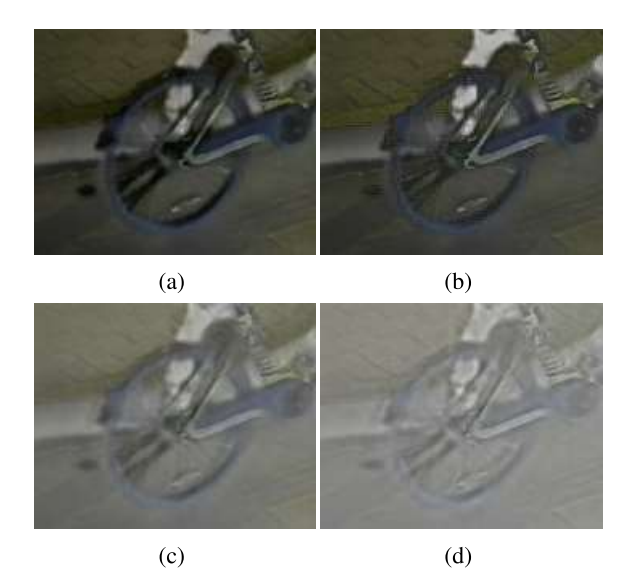


Figure 4: Detail of the resulting image for the averaged and max-value fusion. (a) Wavelet average fusion. (b) Wavelet max-value fusion. (c) Curvelet average fusion. (d) Curvelet max-value fusion.

and both frequency-domain based methods (https://github.com/enheragu/yolo_test_utils/blob/v2.1.0-icinco/src/Dataset/fusion_methods/wavelets_mdmr_compression.py, accessed on 01 July 2025) are publicly available.

4 **RESULTS**

Table 2: Summary of the average computation time to perform the fusion for each of the methods based on the images from the LLVIP dataset.

Fusion Method	Mean (s)	Std (s)
PCA Fusion	0.9630	0.2030
FA Fusion	62.9443	11.9214
Wavelet Fusion	0.8314	0.0664
Curvelet Fusion	68.8148	2.2531

As already mentioned, although mAP (mean Average Precision) is the standard when comparing different detection deep learning algorithms, specific use case might require a more in depth analysis. In this research precision and recall are evaluated alone, and then both mAP50 and mAP50-95 are presented.

Figure 5 depicts a precision recall curve for each of the methods. Note that the axis have been adjusted to focus the plot on the area of interest.

 As it can be seen, although the FA method (the yellow line in the graph) reaches the highest precision, the recall slightly degrades. As indicated in the Introduction, this research is focused on SAR

	*				<i>c c</i>
Method	Precision	Recall	mAP50	mAP50-95	Best Epoch
Visible alone	0.871	0.799	0.870	0.487	18
LWIR alone	0.961	0.914	0.966	0.655	37
VT (No eq.)	0.946	0.900	0.955	0.640	16
VT (Thermal eq.)	0.961	0.935	0.974	0.671	60
PCA Fusion	0.9602	0.9107	0.9589	0.6416	36
FA Fusion	0.9659	0.9070	0.9582	0.6368	37
Wavelet Fusion (mean)	0.9606	0.8899	0.9543	0.6405	38
Wavelet Fusion (max)	0.9525	0.8827	0.9454	0.6289	58
Curvelet Fusion (mean)	0.9537	0.8858	0.9476	0.6066	15
Curvelet Fusion (max)	0.9612	0.8602	0.9346	0.6190	64

Table 3: Detection performance (mAP) and fusion time for each method compared to Visible, LWIR and VT method (Heredia-Aguado et al., 2025) with thermal channel equalization. The most relevant results are highlighted in bold.

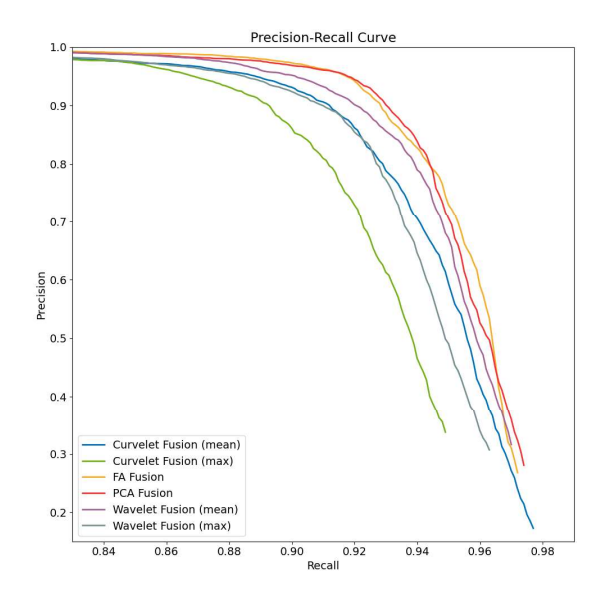


Figure 5: Precision recall curve for all the methods included in this research.

operations or vigilance, areas in which missing instances might be more critical than in other domains. For this reason, it is always advisable to operate at a work point with a high recall, rather than a high precision.

- With a similar behaviour, the Curvelet with maxvalue (green line in the graph) fusion also reaches a high precision before quickly deteriorating. In this sense, the mean-fusion version of the Curvelet (blue line in the plot) approach although starting with a lower precision, it is capable of maintaining a better recall, which would make it more suitable for SAR operations.
- On the other hand, methods like the Wavelet fusion (mean) (purple line) and PCA (red line), fusion demonstrate a more balanced performance, maintaining relatively high precision even as recall increases. From the Table 3, PCA fusion con-

sistently achieves the best mAP50 and mAP50-95 from the methods discussed in this article.

• Finally the maximum-value version of the Wavelet fusion has a similar behaviour than the max-value version of the Curvelet fusion method. Although the mean-value version of the Curvelet fusion method has a more balanced performance than both max-value fusion (wavelet and curvelet) it is still quite low in performance both in precision and recall, as seen in Table 3, compared to the other methods (mean-version of the Wavelet fusion, PCA and FA fusions.

Although precision and recall are an important metric, execution time should not be forgotten. In Table 2 a summary of fusion time for each method is presented. As it can be observed, Factor Analysis and Curvelet approach are quite time consuming methods, taking more than one minute for each image, while PCA and Wavelet fusion takes less than one second, complying with the 1 Hz requirement mentioned in the introduction. Note that the images in the LLVIP dataset are quite big in terms of resolution, these methods might be faster under other circumstances as working with images from the KAIST dataset, that are half the pixel size with regards to the LLVIP dataset images.

Table 3 summarizes the detection results for all fusion methods, as well as single-modality baselines (RGB-only, LWIR-only), using metrics from our previous work (Heredia-Aguado et al., 2025) for reference. Based on a visual inspection of the dataset images from Figure 2 it can be already advanced that the visible channel would have a low performance as it includes pretty poor information. On the other hand the LWIR/Thermal images has the largest quantity of information, compared to RGT images due to the nature of the dataset involved in the tests (daylight images could differ). Due to the invariance in pedestrian temperature and the low temperature of the background

at night, pedestrians are well defined, which already advances a good performance based on this information. These results can be compared to the VT fusion method (Heredia-Aguado et al., 2025), presented in the table, and tested under the same conditions as the rest of the methods described in this manuscript (night condition based on LLVIP dataset). The poor colour information that can be observed explains the performance of the VT method (Heredia-Aguado et al., 2025) as it is based on combining the intensity channel from the RGB image with the thermal channel from the LWIR image, disregarding the colour information. Note that this method includes an equalization of the thermal channel, that proved to be relevant in enhancing the results of the methods tested, as the non equalized version performed poorly with regards to the presented methods (Heredia-Aguado et al., 2025). In terms of mAP50 and mAP50-95 both PCA fusion and FA fusion seem to be promising, and might benefit a lot from a thermal channel equaliza-

Table 2 showed the average computation time of each fusion method. Once the image has been fused it is fed to the detection algorithm, YOLOv8, to be trained on this specific image set. It is important to review the difficulties the network might have to reach the best performance, depicted in Figure 5, on each image fusion type. In terms of training duration, PCA, FA, and Wavelet fusion methods all achieved similar performance within a comparable number of epochs. The LWIR-alone approach also required a similar training time, whereas the VT fusion method needed almost twice as many epochs to reach its best result. Notably, the results from both the equalized and non-equalized versions of VT fusion indicate that applying an equalization phase increases the training time required for all methods, but also leads to improved performance.

4.1 Discussion

Despite the sophistication of the dynamic fusion methods, improvements with regards to previous and simpler fusion methods are limited on LLVIP, likely due to the dataset's high image quality and lack of challenging occlusions.

Notably, mean-based fusion in Wavelets outperformed max-value based fusion for detail coefficients, suggesting that averaging may better preserve subtle features in detection tasks for this specific use case. In the case of the Curvelet fusion, although the precision was improved, the recall suffered a relevant drop in terms of recall. Contrary to some of the bibliography already presented, mean-based fusion proved to

be more balanced for detection tasks based on RGB-Thermal image fusion.

Although both Factor Analysis (FA) and Curveletbased fusion methods offer theoretically appealing approaches for extracting and combining complementary information from RGB and thermal images, their practical application in this study revealed significant practical limitations due to computational speed. In our experiments, these methods proved to be considerably slower than other fusion strategies, making them less suitable for real-time deployment scenarios, such as onboard robotic systems for search and rescue or surveillance. The high computational cost associated with FA and Curvelet transforms, particularly during the transformation and inverse reconstruction stages, poses a substantial bottleneck, especially when compared to more efficient methods like PCA or deep learning-based early fusion. This tradeoff must be carefully considered when selecting fusion algorithms for time-sensitive applications.

5 CONCLUSIONS

We present a robust comparative study of dynamic fusion methods for RGB and thermal images, evaluated with YOLOv8 on LLVIP dataset. While advanced methods do not always outperform simpler baselines in controlled settings, our work underscores the importance of methodological rigour and transparent reporting of negative results. Such studies are essential for advancing the state of the art and guiding future research in multispectral fusion.

It is important to note that the presented study is limited to well-aligned, high-quality images. Future work should evaluate fusion methods on more challenging datasets, including occlusions, or diverse environmental conditions.

As already mentioned, it is important to evaluate these methods with different equalization techniques, as it proved to be relevant with early fusion methods for the detection task (Heredia-Aguado et al., 2025). Future work should take this into account. Although under the conditions described, the methods were not able to outperform LWIR alone or VT (with thermal equalization), the results from VT without equalization suggest that there is potential for improvement with better fusion strategies.

ACKNOWLEDGEMENTS

This research work is part of the project funded by "AYUDAS A LA INVESTIGACIÓN 2025

DEL VICERRECTORADO DE INVESTIGACIÓN Y TRANSFERENCIA" of the Miguel Hernández University; the project PID2023-149575OB-I00 funded by MICIU/AEI/10.13039/501100011033 and by FEDER, UE; and the project CIPROM/2024/8, funded by Generalitat Valenciana, Conselleria de Educación, Cultura, Universidades y Empleo (program PROMETEO 2025).

REFERENCES

- Carion, N., Massa, F., Synnaeve, G., Usunier, N., Kirillov, A., and Zagoruyko, S. (2020). End-to-end object detection with transformers. In Vedaldi, A., Bischof, H., Brox, T., and Frahm, J.-M., editors, *Computer Vision ECCV 2020*, pages 213–229, Cham. Springer International Publishing.
- Diwan, T., Anirudh, G., and Tembhurne, J. V. (2023). Object detection using yolo: challenges, architectural successors, datasets and applications. *Multimedia Tools and Applications*, 82(6):9243–9275.
- Elmasry, S. A., Awad, W. A., and Abd El-hafeez, S. A. (2020). Review of different image fusion techniques: Comparative study. In Ghalwash, A. Z., El Khameesy, N., Magdi, D. A., and Joshi, A., editors, *Internet of Things—Applications and Future*, pages 41–51, Singapore. Springer Singapore.
- Heredia-Aguado, E., Cabrera, J. J., Jiménez, L. M., Valiente, D., and Gil, A. (2025). Static early fusion techniques for visible and thermal images to enhance convolutional neural network detection: A performance analysis. *Remote Sensing*, 17(6).
- Hwang, S., Park, J., Kim, N., Choi, Y., and Kweon, I. S. (2015). Multispectral pedestrian detection: Benchmark dataset and baseline. In 2015 IEEE Conference on Computer Vision and Pattern Recognition (CVPR), pages 1037–1045.
- Indira, K. (2015). Image fusion for pet ct images using average maximum and average contrast rules. *Int J Appl Eng Res*, 10(1):673–80p.
- Jia, X., Zhu, C., Li, M., Tang, W., and Zhou, W. (2021). Llvip: A visible-infrared paired dataset for low-light vision. In *Proceedings of the IEEE/CVF International* Conf. on Computer Vision, pages 3496–3504.
- Jiang, P., Ergu, D., Liu, F., Cai, Y., and Ma, B. (2022). A review of yolo algorithm developments. *Procedia Computer Science*, 199:1066–1073. The 8th International Conference on Information Technology and Quantitative Management (ITQM 2020 & 2021): Developing Global Digital Economy after COVID-19.
- Jocher, G., Chaurasia, A., and Qiu, J. (2023). YOLOv8 by Ultralytics.
- Joliffe, I. and Morgan, B. (1992). Principal component analysis and exploratory factor analysis. *Statistical Methods in Medical Research*, 1(1):69–95. PMID: 1341653.
- Kumar, S. S. and Muttan, S. (2006). PCA-based image fusion. In Shen, S. S. and Lewis, P. E., editors,

- Algorithms and Technologies for Multispectral, Hyperspectral, and Ultraspectral Imagery XII, volume 6233, page 62331T. International Society for Optics and Photonics, SPIE.
- Ma, J. and Plonka, G. (2010). The curvelet transform. *IEEE Signal Processing Magazine*, 27(2):118–133.
- McInnes, L., Healy, J., and Melville, J. (2020). Umap: Uniform manifold approximation and projection for dimension reduction.
- Ofir, N. (2023). Multispectral image fusion based on super pixel segmentation. In *ICASSP 2023 2023 IEEE International Conf. on Acoustics, Speech and Signal Processing (ICASSP)*, pages 1–5.
- Patil, V., Sale, D., and Joshi, M. (2013). Image fusion methods and quality assessment parameters. *Asian Journal of Engineering and Applied Technology*, 2:40–45.
- Ren, S., He, K., Girshick, R., and Sun, J. (2017). Faster r-cnn: Towards real-time object detection with region proposal networks. *IEEE Transactions on Pattern Analysis and Machine Intelligence*, 39(6):1137–1149.
- Sahu, V. and Sahu, D. (2014). Image fusion using wavelet transform: A review. *Global Journal of Computer Science and Technology*, 14(F5):21–28.
- Sifuzzaman, M., Islam, R., and Ali, M. (2009). Application of wavelet transform and its advantages compared to fourier transform. *Journal of Physical Science*, 13:121–134.
- Starck, J.-L., Candes, E., and Donoho, D. (2002). The curvelet transform for image denoising. *IEEE Transactions on Image Processing*, 11(6):670–684.
- Van der Maaten, L. and Hinton, G. (2008). Visualizing data using t-SNE. *Journal of machine learning research*, 9(11).
- Zhang, D. (2019). Wavelet Transform, pages 35–44. Springer International Publishing, Cham.